Closed-loop input impedance of PWM buck-derived DC-DC convertersProceedings of IEEE International Symposium on Circuits

Closed–Loop Input Impedance of PWM Buck–Derived DC–DC Converters

Marian K. Kazimierczuk, Robert C. Cravens, II
Wright State University
Department of Electrical Engineering
Dayton, OH 45435, U. S. A.

Alberto Reatti
Universty of Florence
Department of Electronic Engineering
50139 Florence, Italy

***Abstract*— The small–signal closed–loop input impedance is derived for the PWM buck dc–dc converter operated in continuous conduction mode (CCM), taking into account all parasitic resistances. The plots of the closed–loop input impedance are shown versus frquency for four values of the equivalent series resistance of the capacitor.** [1]

I. INTRODUCTION

A small–signal linear circuit model of the PWM buck converter has been developed, taking into account all parasitic resistances [1]–[3]. This derivation used an evergy conservation method. The current ripple in the inductor is neglected in [1], [2] and is taken into account in [3]. Open–loop small–signal characteristics were illustrated using this model. The purpose of this paper is to present the derivation of the closed–loop input impedance of the voltage–mode–controlled PWM buck dc–dc power converter with a proportional controller for CCM.

II. SMALL–SIGNAL CIRCUIT MODEL OF THE PWM BUCK CONVERTER

A circuit of the PWM buck converter is shown in Fig. 1(a). It consists of a power MOSFET as a switch S, a diode $D1$, an inductor L, and a filter capacitor C. The converter is fed by a dc input voltage source V_I and is loaded by a dc load resistance R. The switch is turned on and off at the switching frequency $f_s = 1/T$ and the on–duty ratio is $D = t_{on}/T$, where t_{on} is the time interval during which the switch is on. Parasitic components associated with each circuit component, where r_{DS} is the MOSFET's on-resistance, R_F is the diode forward resistance, V_F is the diode threshold voltage, r_L is the equivalent series resistance of inductor L, and r_C is the ESR of the filter capacitor C.

Fig. 1(b) depicts a small–signal model of this converter [1], where d is the ac component of the switch duty ratio, v_i is the ac component of the input voltage, v_o is the ac component of the output voltage, I_L is the dc component of the inductor current, and i_l is the ac component of the inductor current. Resistance r is an equivalent averaged resistance (EAR) and is given by [1]

$$r = Dr_{DS} + (1 - D)R_F + r_L. \qquad (1)$$

Fig. 1(c) shows a block diagram of a closed–loop buck converter. T_p represents a small–signal model of the buck

[1]This work was supported by the National Science Foundation under Grant ECS–8922695.

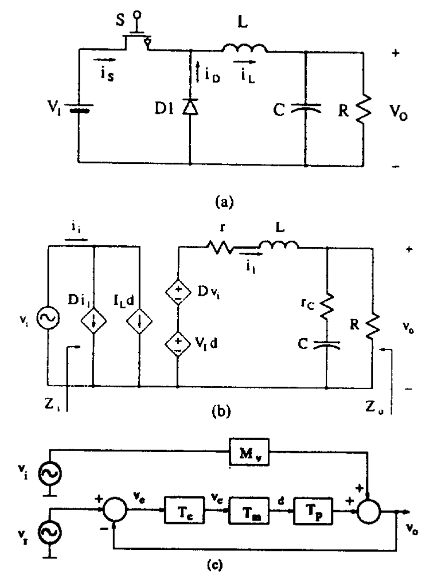

Fig. 1: PWM buck converter. (a) Circuit. (b) Small–signal model (c) Block diagram of the closed–loop voltage–mode–controlled converter.

converter, T_m represents a PWM modulator, T_c represents a controller, M_v represents an input–to–output voltage transfer function, T_{ol} is the the open–loop control–to–output transfer function, v_c is the output voltage of the controller, v_e is the error signal applied to the input of the controller, and v_r is the ac component of the reference voltage. This is a two–input and a single–output system. It is driven by two independent sources, v_r and v_i. The ac component of the output voltage is

$$v_o(s) = \frac{T_{ol}}{1 + T_{ol}} v_r(s) + \frac{M_v(s)}{1 + T_{ol}} v_i(s). \qquad (2)$$

The PWM buck–derived converters such as the forward, push–pull, half–bridge, and full–bridge converters (which contain transformers) have the same small–signal model and characteristics as the PWM buck converter [2]. Therefore, the transformer turns ratio n is included in the subsequent equations. The equivalent averaged resistance r is the only difference between these converters [2].

III. OPEN–LOOP TRANSFER FUNCTIONS

The small–signal model of Fig. 1(b) can be used to describe the converter performance for frequencies f up to about one-half the switching frequency f_s. Using this model, one can derive the ***control-to-output*** (or ***duty ratio-to-output***) ***transfer function*** in the s-domain

$$T_p(s) \equiv \frac{v_o(s)}{d(s)} \, |_{v_i(s)=0}$$

$$= \frac{V_I R r_C}{nL(R+r_C)} \frac{s + \frac{1}{Cr_C}}{s^2 + s\frac{C(Rr_C+Rr+r_Cr)+L}{LC(R+r_C)} + \frac{R+r}{LC(R+r_C)}}$$

$$= \frac{V_I R \omega_r^2}{n\omega_z(R+r)} \frac{s+\omega_z}{s^2 + 2\xi_r\omega_r s + \omega_r^2} \qquad (3)$$

where the frequency of the zero is

$$\omega_z = \frac{1}{Cr_C} \qquad (4)$$

the corner frequency is

$$\omega_r = \sqrt{\frac{R+r}{LC(R+r_C)}} \qquad (5)$$

and the damping ratio is

$$\xi_r = \frac{C(Rr_C + Rr + r_Cr) + L}{2\sqrt{LC(R+r_C)(R+r)}}. \qquad (6)$$

Fig. 2(a) and (b) shows plots of the magnitude and the phase of T_p. The characteristics of T_p are plotted for four values of r_C because they strongly depend on r_C.

The voltage transfer function of the PWM modulator is

$$T_m \equiv \frac{d(s)}{v_c(s)} = \frac{1}{V_{Tm}} \qquad (7)$$

where V_{Tm} is the peak value of the ramp voltage of the PWM modulator. It is assumed that $V_{Tm} = 5$ V, resulting in $T_m = 0.2 = -14$ dB.

The control-to-output transfer function of the converter and the modulator is given by

$$T_1(s) \equiv \frac{v_o(s)}{v_c(s)} = T_m T_p(s)$$

$$= \frac{V_I R \omega_r^2}{n\omega_z V_{Tm}(R+r)} \frac{s+\omega_z}{s^2 + 2\xi_r\omega_r s + \omega_r^2}. \qquad (8)$$

Fig. 2(c) depicts a Bode plot of $|T_1|$. The phase shift ϕ_{T1} of T_1 is the same as the phase shift ϕ_{Tp} and is depicted in Fig. 2(b).

To obtain a wide bandwidth of the open-loop transfer function, a proportional controller is used. The controller which employs an inverting op-amp is shown in Fig. 3. Since the operation at high frequencies is of interest, the frequency response of the op-amp should be taken into account. For this reason, a pure proportional controller is difficult to realize. The voltage transfer function of the controller for the ac component is

$$T_c(s) \equiv \frac{v_c(s)}{v_e(s)} = \frac{A_{vo}}{1 + \frac{s}{\omega_{Hf}}} = \frac{A_{vo}}{1 + \frac{sA_{vo}}{\omega_1}} \qquad (9)$$

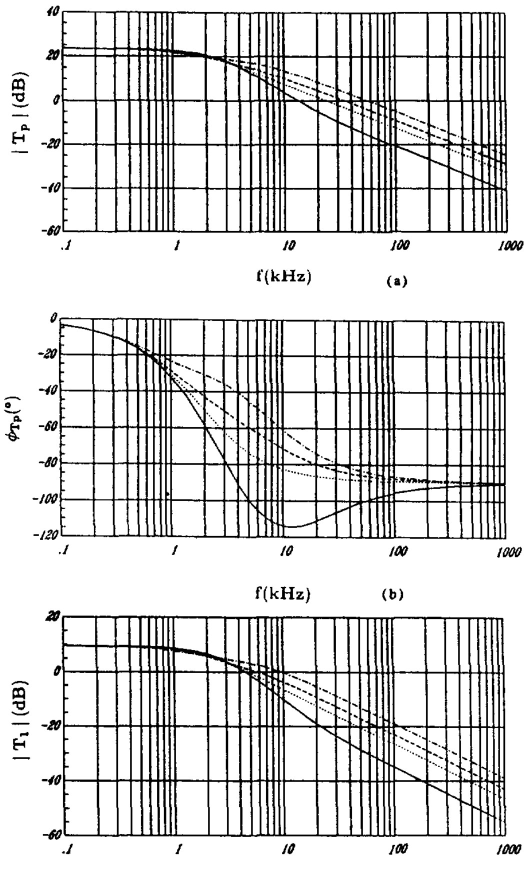

Fig. 2: Control-to-output transfer function $T_p = |T_p| e^{j\phi_{T_p}}$ and $|T_1|$ for $V_I = 30$ V, $n = 1$, $L = 5$ μH, $C = 1$ mF, $R = 0.25$ Ω, $r = 0.15$ Ω, $D = 0.3$, and various values of $r_C = 0.01$ (solid line), 0.03, 0.05, and 0.1 Ω. (a) $|T_p|$ against f. (b) $\phi_{T_p} = \phi_{T_1}$ against f. (c) $|T_1|$ against f.

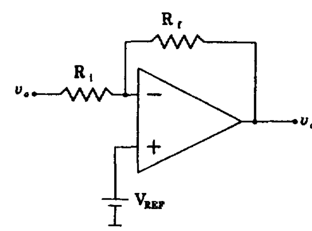

Fig. 3: Circuit diagram of the proportional controller.

where the low frequency gain is

$$A_{vo} = \frac{R_f}{R_i}. \qquad (10)$$

The open-loop control-to-output transfer function is

$$T_{ol}(s) = T_c(s)T_1(s) = T_c(s)T_m T_p(s). \qquad (11)$$

Plots of T_{ol} are shown in Fig. 4. The crossover frequency f_c of the open-loop transfer function $|T_{ol}|$ is 27 to 100 kHz

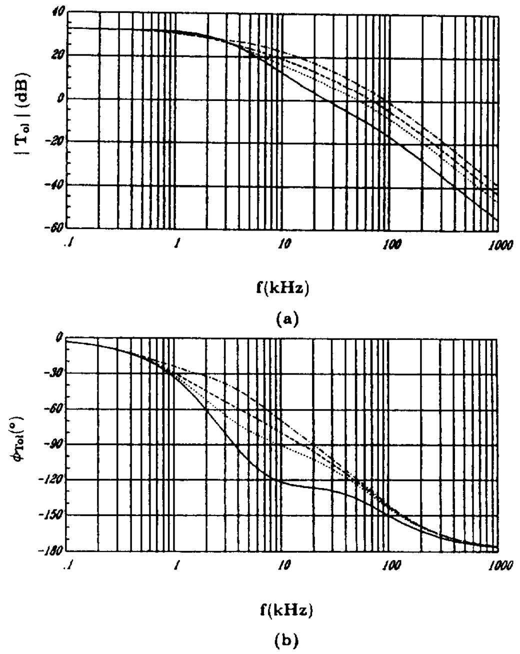

Fig. 4: Open–loop transfer function $T_{ol} = | T_{ol} | e^{j\phi_{T_{ol}}}$ for $L = 5\ \mu$H, $C = 1$ mF, $R = 0.25\ \Omega$, $r = 0.15\ \Omega$, $D = 0.3$, $A_{vo} = 14$, and various values of $r_C = 0.01$ (solid line), 0.03, 0.05, and 0.1 Ω. (a) $| T_{ol} |$ against f. (b) $\phi_{T_{ol}}$ against f.

for r_C ranging from 0.01 to 0.1 Ω. The phase margin is greater than 45°. Since the phase $\phi_{T_{ol}}$ never crosses −180°, the gain margin cannot be determined.

The ***input–to–output*** (or ***line–to–output***) ***voltage transfer function*** (which describes the input–output noise transmission), is

$$M_v(s) \equiv \frac{v_o(s)}{v_i(s)} \,|_{d(s)=0}$$

$$= \frac{DRr_C}{nL(R+r_C)} \frac{s + \frac{1}{Cr_C}}{s^2 + s\frac{C(Rr_C+Rr+r_Cr)+L}{LC(R+r_C)} + \frac{R+r}{LC(R+r_C)}}$$

$$= \frac{DR\omega_r^2}{n\omega_z(R+r)} \frac{s+\omega_z}{s^2 + 2\xi_r\omega_r s + \omega_r^2}. \qquad (12)$$

It follows from (12) that $| M_v |$ increases with increasing D. Therefore, M_v should be considered for the maximum value of D. Plots of $| M_v |$ are shown in Fig. 5.

The ***open–loop input impedance*** is

$$Z_i(s) \equiv \frac{v_i(s)}{i_i(s)} \,|_{d(s)=0}$$

$$= \frac{n^2L}{D^2} \frac{s^2 + s\frac{C(Rr_C+Rr+r_Cr)+L}{LC(R+r_C)} + \frac{R+r}{LC(R+r_C)}}{s + \frac{1}{C(R+r_C)}}$$

$$= \frac{n^2L}{D^2} \frac{s^2 + 2\xi_r\omega_r s + \omega_r^2}{s+\omega_{cr}} \qquad (13)$$

where

$$\omega_{cr} = \frac{1}{C(R+r_C)}. \qquad (14)$$

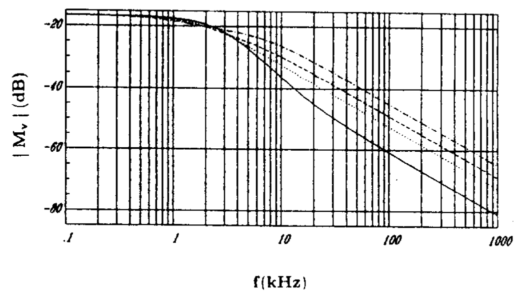

Fig. 5: Magnitude of the open–loop input–to–output transfer function $| M_v |$ against f for $V_I = 30$ V, $n = 1$, $L = 5\ \mu$H, $C = 1$ mF, $R = 0.25\ \Omega$, $r = 0.15\ \Omega$, $D = 0.3$, and various values of $r_C = 0.01$ (solid line), 0.03, 0.05, and 0.1 Ω.

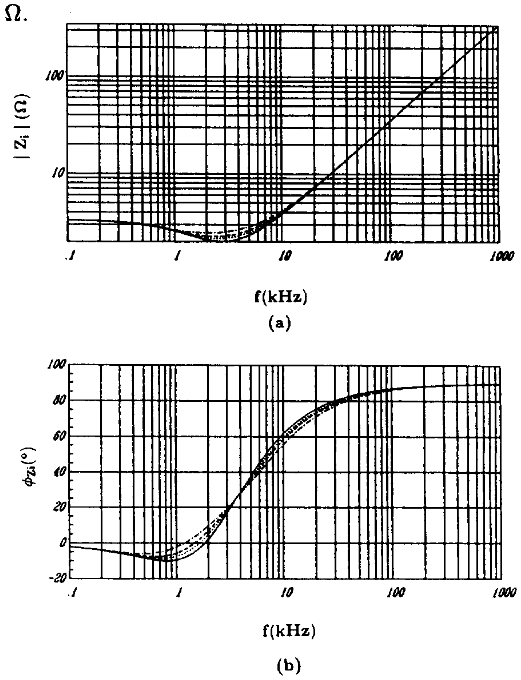

Fig. 6: Open–loop input impedance $Z_i = | Z_i | e^{j\phi_{Z_i}}$ for $D = 0.3$, $n = 1$, $L = 5\ \mu$H, $C = 1$ mF, $R = 0.25\ \Omega$, $r = 0.15\ \Omega$, $D = 0.3$, and various values of $r_C = 0.01$ (solid line), 0.03, 0.05, and 0.1 Ω. (a) $| Z_i |$ against f. (b) ϕ_{Z_i} against f.

For $s = 0$,

$$Z_i(0) = \frac{n^2(R+r)}{D^2}. \qquad (15)$$

Fig. 6 shows plots of Z_i as a function of frequency.

IV. CLOSED–LOOP INPUT IMPEDANCE

The closed–loop input impedance can be derived as follows. Referring to the block diagram shown in Fig. 1(c) and assuming $v_r = 0$,

$$v_o = T_p d + M_v v_i \qquad (16)$$

$$d = -v_o T_c T_m = -(T_p d + M_v v_i) T_c T_m. \qquad (17)$$

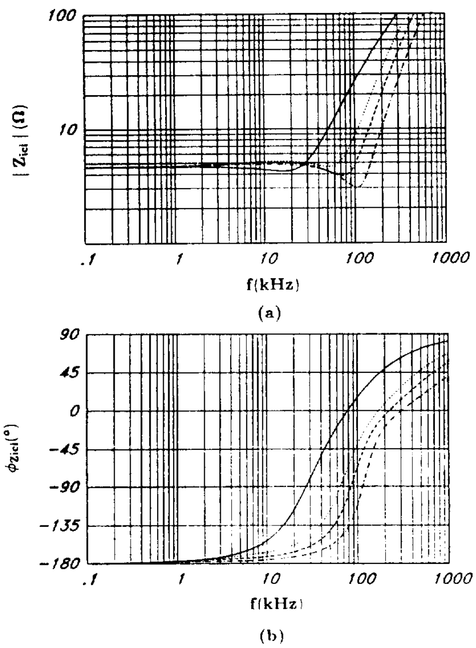

Fig. 7: Closed-loop input impedance $Z_{icl} = | Z_{icl} | e^{j\phi_{Zicl}}$ for $A_{vo} = 14$, $f_1 = 1$ MHz, $V_{Tm} = 5$ V, $D = 0.3$, $n = 1$, $L = 5$ μH, $C = 1$ mF, $R = 0.25$ Ω, $r = 0.15$ Ω, $D = 0.3$, and various values of $r_C = 0.01$ (solid line), 0.03, 0.05, and 0.1 Ω. (a) $| Z_{icl} |$ against f. (b) ϕ_{Zicl} against f.

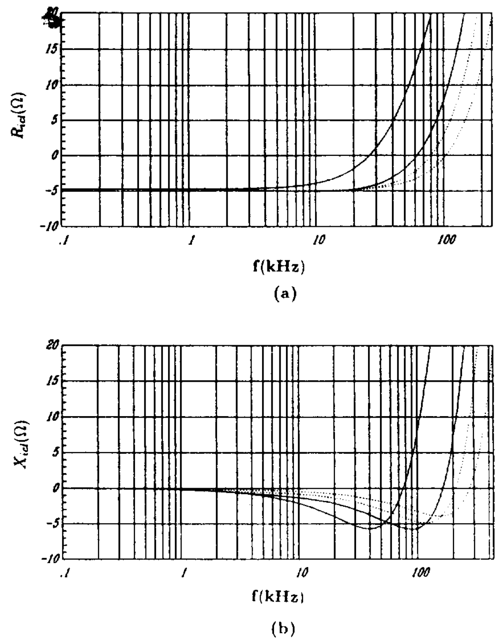

Fig. 8: Closed-loop input impedance $Z_{icl} = R_{icl} + jX_{icl}$ for $A_{vo} = 14$, $f_1 = 1$ MHz, $V_{Tm} = 5$ V, $D = 0.3$, $n = 1$, $L = 5$ μH, $C = 1$ mF, $R = 0.25$ Ω, $r = 0.15$ Ω, $D = 0.3$, and various values of $r_C = 0.01$ (solid line), 0.03, 0.05, and 0.1 Ω. (a) R_{icl} against f. (b) X_{icl} against f.

Dividing (12) by (3) gives

$$M_v = \frac{D}{V_I} T_p. \tag{18}$$

Substitution of (11) and (18) into (17) yields

$$d = -\frac{T_c T_m M_v}{1 + T_c T_m T_p} v_i = -v_i \left(\frac{M_v}{T_p}\right)\left(\frac{T_{ol}}{1 + T_{ol}}\right)$$
$$= -\frac{D T_{ol}}{V_I (1 + T_{ol})} v_i. \tag{19}$$

Neglecting V_F in a dc model of the buck converter [1],

$$I_L = \frac{D V_I}{n(R + r)}. \tag{20}$$

Finally, the closed-loop input admittance is given by

$$Y_{icl} = \frac{1}{Z_{icl}} \equiv \frac{i_i}{v_i} = \frac{D i_l + I_L d}{n v_i}$$
$$= \frac{1}{Z_i} \frac{1}{1 + T_{ol}} - \frac{D I_L}{V_I} \frac{T_{ol}}{1 + T_{ol}}$$
$$= \frac{1}{Z_i} \frac{1}{1 + T_{ol}} - \frac{D^2}{n^2 (R + r)} \frac{T_{ol}}{1 + T_{ol}} \tag{21}$$

where $i_l = n(D v_i + V_I d)/(D^2 Z_i)$. If $s = 0$ and $| T_{ol} | >> 1$ then

$$Z_{icl}(0) \approx -\frac{n^2 (R + r)}{D^2} = -Z_i(0). \tag{22}$$

For $f >> f_c$ and $| T_{ol} | << 1$, $Z_{icl} \approx Z_i(1 + T_{ol}) \approx Z_i$. Figs. 7 and 8 show plots of the closed-loop input impedance. It can be seen from Fig. 8(a) that the closed-loop input resistance R_{icl} is negative at low frequencies.

V. CONCLUSIONS

The small-signal closed-loop input impedance of the PWM buck-derived dc-dc power converters has been derived and illustrated for four values of the ESR of the filter capacitor. A proportional controller was used. Plots of the closed-loop input-impedance have been shown. The closed-loop input resistance is negative at low frequencies. The results agree with those obtained from the state-space averaging method [4].

REFERENCES

[1] D. Czarkowski and M. K. Kazimierczuk, "Circuit models of PWM dc-dc converters," *Proceedings of the IEEE Nat. Aerospace and Electronic Systems Conference (NAECON'92)*, Dayton, OH, May 18–22, 1992, pp. 407–413.

[2] D. Czarkowski and M. K. Kazimierczuk, "Static- and dynamic-circuit models of PWM buck-derived dc-dc converters," *IEE Proceedings, Pt. G, Circuits, Devices and Systems*, vol. 139, pp. 669–679, Dec. 1992.

[3] D. Czarkowski and M. K. Kazimierczuk, "Energy-conservation approach to modeling PWM DC-DC converters," *IEEE Transactions on Aerospace and Electronic Systems*, vol. 29, pp. 1059–1063, July 1993.

[4] R. D. Middlebrook and S. Ćuk, *Advances in Switched-Mode Power Conversion*, vols. I and II. Pasadena, CA, TESLAco, 1981.